Available online at www.sciencedirect.com
ScienceDirect
Surface Science 601 (2007) 4370–4374
SURFACE SCIENCE
www.elsevier.com/locate/susc

Structural and magnetic properties of Mn_5Ge_3 nanoclusters dispersed in Mn_xGe_{1-x}/Ge(001)2 × 1 diluted magnetic semiconductors

P. De Padova [a,*], L. Favre [b], I. Berbezier [b], B. Olivieri [c], A. Generosi [a], B. Paci [a], V. Rossi Albertini [a], P. Perfetti [a], C. Quaresima [a], J.-M. Mariot [d], A. Taleb-Ibrahimi [e], M.C. Richter [f], O. Heckmann [f], F. D'Orazio [g], F. Lucari [g], K. Hricovini [f]

[a] CNR-ISM, via Fosso del Cavaliere, 00133 Roma, Italy
[b] L2MP – Technopôle de Château – Gombert, 13451 Marseille Cedex 20, France
[c] CNR-ISAC, via Fosso del Cavaliere, 00133 Roma, Italy
[d] LCPMR (UMR 7614), Université Pierre et Marie Curie, 11 rue P. et M. Curie, 75005 Paris, France
[e] Synchrotron SOLEIL, L'Orme des Merisiers, Saint Aubin, BP 48, 91192 Gif sur Yvette, France
[f] LPMS, Université de Cergy-Pontoise, Neuville/Oise, 95031 Cergy-Pontoise, France
[g] INFM-Dipartimento di Fisica, Università di L'Aquila, via Vetoio-Coppito, I-67010 L'Aquila, Italy

Available online 16 June 2007

Abstract

We investigated the structural and magnetic properties of Mn_xGe_{1-x}, with $0.02 \leqslant x \leqslant 0.1$. The Mn_xGe_{1-x} samples were grown on Ge(001)2 × 1 by molecular beam epitaxy, at a substrate temperature of 520 K. The samples were characterized *in situ* by reflection high-energy electron diffraction and *ex situ* by high-resolution transmission electron microscopy, energy dispersive X-ray reflectivity and magneto-optical Kerr effect. From microscopy images we evidenced on all samples the presence of Mn_5Ge_3 nanocrystallites in addition to the Mn_xGe_{1-x} diluted magnetic semiconductor with an estimated Mn concentration $x \approx 1.5\%$. The size and the density of the Mn_5Ge_3 precipitates were found to increase with increasing the Mn concentration x. Magnetic analysis showed ferromagnetism with a Curie temperature of 280 K for all samples.

Keywords: MnGe diluted magnetic semiconductor; Mn_5Ge_3 nanoclusters; HRTEM; EDXR; MOKE

1. Introduction

Diluted magnetic semiconductors (DMS) [1,2] with high carrier spin-polarization can be synthesized by molecular beam epitaxy (MBE) in semiconductor layer structures exhibiting a very rich magnetic behavior as a function of the chemical composition [3]. Understanding and controlling the spin interactions as well as the roles of defects, dimensionality, and semiconductor host are key elements to develop efficient spin-based electronic devices. Different theoretical models, based on the double exchange model and Zener's p–d exchange interaction, have been proposed to explain ferromagnetic (FM) coupling among 3d impurities in semiconducting hosts [3–5]. All present theories, however, do not correctly account for the observed magnetization, which is lower than what is expected from the estimate of the local impurity moments. Several evidences suggest that the magnetic properties of the DMS are often significantly influenced by the presence of 3d impurities in non-substitutional sites, as metal clusters, interstitial and antisite defects, which cannot be sufficiently controlled or suppressed in the growth process.

Magnetic Mn–Ge systems have recently attracted much attention due to the possibility to elaborate DMSs with high Curie temperatures (T_C) (see Ref. [2]) and to integrate them on Si devices. However, the question whether the ferromagnetism of Mn–Ge systems comes from DMSs or

* Corresponding author. Tel.: +39 06 4993 4144; fax: +39 06 4993 4153.
E-mail address: depadova@ism.cnr.it (P. De Padova).

0039-6028/$ - see front matter © 2007 Elsevier B.V. All rights reserved.
doi:10.1016/j.susc.2007.06.020

from magnetic precipitates [6,7] is still under intense debate. It is interesting to note that Mn and Ge atoms can combine to form various stable precipitates as a function of temperature [6–13]. These precipitates can contribute to the magnetic properties. The most stable precipitate is Mn_5Ge_3 with a T_C of 310 K [14]. Mn_5Ge_3 films grow epitaxially on Ge(1 1 1) [15], whereas formation of Mn_5Ge_3 precipitates takes place on Ge(0 0 1) if the substrate temperature (T_S) is high enough [10–13].

In this paper we report on a study of the structural and magnetic properties of Mn_xGe_{1-x} films, with $x = 0.02-0.1$, grown by MBE on Ge(0 0 1)2×1 substrate. The growth was investigated by high-resolution transmission electron microscopy (HRTEM) and by selected-area electron diffraction (SAED). Energy dispersive X-ray reflectivity (EDXR) provided the roughness, thickness and scattering length density (SLD) of the alloys. Magneto-optical Kerr effect (MOKE) measurements have been used to explore the magnetic properties of the Mn_xGe_{1-x} alloys.

2. Experimental

The Mn_xGe_{1-x} alloys ($0.02 \leqslant x \leqslant 0.1$) were grown on the reconstructed Ge(0 0 1)2×1 surface by co-evaporating Mn and Ge at a low growth rate using MBE Knudsen cell sources and keeping the substrate temperature at 520 K. T_S was measured by an infrared pyrometer and the film thickness by a quartz microbalance. Reflection high-energy electron diffraction was used *in situ* to monitor the growth of the films. In order to perform *ex situ* measurements, a thin Ge layer was deposited on the surface of the samples. HRTEM cross-sectional images were collected with a microscope (Jeo 2010F) having primary energy beam $E = 200$ keV along the [1 1 0] direction. The energy dispersive reflectometer used consists of a non-commercial instrument equipped with a standard X-ray tube with a W anode and with an ultra pure Ge solid-state detector, cooled by an electromechanical refrigerator and connected to an integrated spectroscopy amplifier-multi channel analyzer system [16]. The measurements were carried out in the reflection geometry at a very low reflection angle in stationary conditions of the apparatus, since in EDXR no movement is required to collect the reflection profiles.

MOKE hysteresis loops were measured in a magnetic field up to 0.56 T in both polar and longitudinal geometries, at various temperatures between 13 K and room temperature, using s-polarized radiation ($\lambda = 1.6$ μm) incident on the film surface at an angle of 45°.

3. Results and discussion

3.1. HRTEM

Fig. 1 shows typical cross-sectional HRTEM images of Mn_xGe_{1-x} samples, with Mn concentration $x = 0.02$ (a), 0.04 (b), 0.06 (c) and 0.1 (d), grown on a Ge(0 0 1) substrate held at $T_S = 520$ K. The incident electron beam direction is parallel to the {1 1 0} zone axis of the Ge substrate. The nominal thickness of the Mn_xGe_{1-x} films is 85 nm for $x = 0.02$ and ≈40 nm for $x = 0.04-0.1$, values confirmed by the EDXR measurements. Each film has been capped with a ≈7 nm thick Ge layer. These thickness values are in good agreement with those measured by HRTEM from Fig. 1.

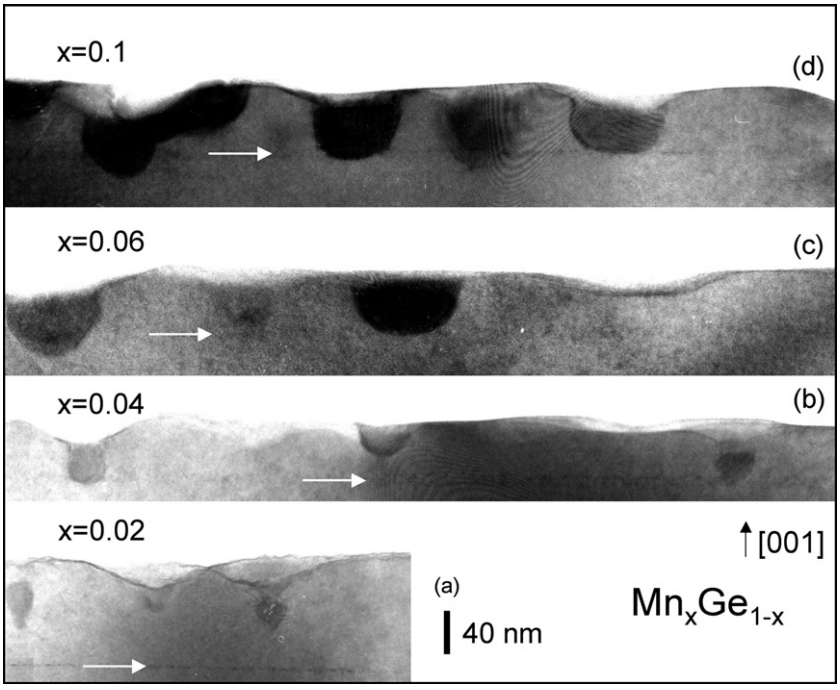

Fig. 1. HRTEM cross-sectional images of Mn_xGe_{1-x} with Mn concentration $x = 0.02$ (a), 0.04 (b), 0.06 (c) and 0.1 (d). The white arrows point out the film–substrate interface.

All the images show the presence in the Mn_xGe_{1-x} epitaxial film of droplet-shaped crystalline clusters. The droplets were indexed as Mn_5Ge_3 precipitates by SAED performed on Mn_xGe_{1-x} for all Mn concentrations x. SAED measurements showed the superposition of two diffraction patterns identified as due to the Ge lattice for the diluted Mn_xGe_{1-x} film and to the Mn_5Ge_3 lattice for the droplet-shaped regions (see Refs. [12,13]). These results are in good agreement with recent findings [10] where, for the growth on a Ge(0 0 1) substrate at $T_S = 495$ K, Mn_5Ge_3 clusters were coherently incorporated in the Mn_xGe_{1-x} DMS matrix with an average Mn concentration of about 2%. In fact, it is well known that the substrate temperature higher than 340 K [7,10] favors the formation of ferromagnetic intermetallic precipitates, e.g., Mn_5Ge_3 [10–13].

The diffraction image in Fig. 2 is obtained by focusing the electron beam in an area containing a crystallite in Mn_xGe_{1-x} with $x = 0.1$. Bright spots are clearly visible, corresponding to the germanium diamond structure, observed in the [1 1 0] direction. The Mn_5Ge_3 diffraction cliché is superimposed, in the axis zone [1 1 $\bar{2}$ 3]. From that we deduce that Ge(3 $\bar{1}$ 1) planes are parallel to Mn_5Ge_3(2 1 $\bar{3}$ 1) planes. Fig. 3 corresponds to a HRTEM image of one crystallite ($x = 0.1$) and its corresponding Fourier transform. The same relationship is observed. No other precipitate phase, for instance $Mn_{11}Ge_8$, has been identified in all samples.

HRTEM images (Fig. 1) show that the Mn_5Ge_3 clusters have mean depth of (30 ± 10) nm (in the {0 0 1} direction), and a maximum width of (60 ± 5) nm (in the {1 1 0} direction). The nanocrytallites observed extend up to the top surface of the layer. Out of the clusters, the very good quality of the epitaxial growth is demonstrated by the perfect alignment of the (1 1 1) planes in the substrate and in the film, and by the absence of impurities and crystalline defects at the interface. The mean size of the Mn_5Ge_3 clusters is found to increase as a function of the Mn concentration x. For $x \leqslant 0.04$, the precipitation of Mn_5Ge_3 does not start immediately at the substrate epilayer interface. Fig. 1a shows that the onset of the precipitation takes place along the growth axis after about 30 nm of Mn_xGe_{1-x} epitaxial film. Figs. 1b–d show that for $x \geqslant 0.04$ the formation of crystallites takes place already at the interface.

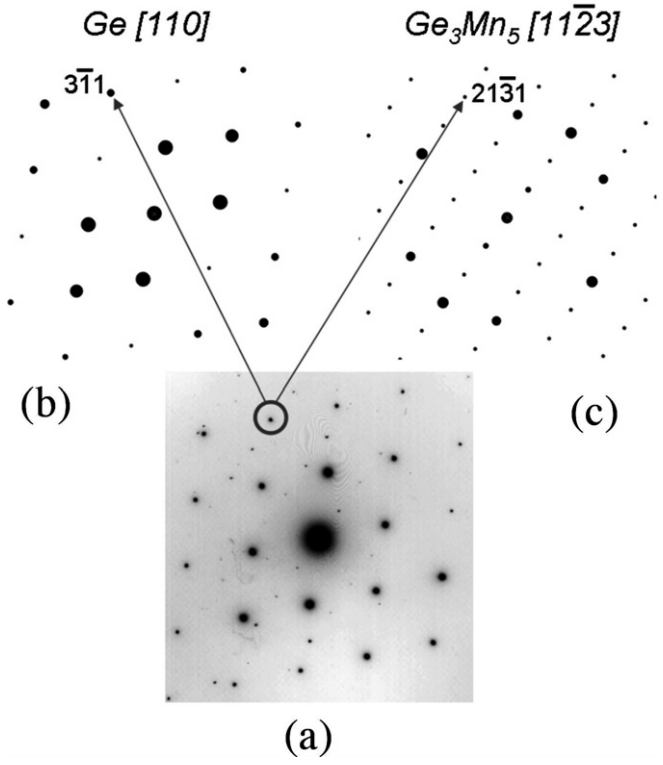

Fig. 2. (a) ED pattern of a cluster in $Mn_{0.1}Ge_{0.9}$ layer. (b) and (c) represent standard diffraction pattern of Ge in [1 1 0] zone axis and Ge_3Mn_5 in [1 1 $\bar{2}$ 3] zone axis, respectively.

In the epitaxial region no contrast is induced by the dilution of Mn in the Ge matrix, which suggests that Mn atoms are mainly incorporated into the Ge crystalline lattice.

Although a quantitative determination of the Mn concentration x at the local Mn_xGe_{1-x} area free from precipitates is quite difficult, a mean value of x can be estimated by evaluating the ratio between the number of Mn atoms incorporated into the Mn_5Ge_3 clusters and the total number of Mn atoms deposited. We find a mean Mn concentration of $\approx$1.5% in the diluted Mn_xGe_{1-x} matrix, a value in agreement with those reported from spatially resolved energy dispersive X-ray spectroscopy measurements [10] and from TEM analysis [12].

From these results, we conclude that Mn_xGe_{1-x} lattice swells up to a critical Mn concentration of $\approx$1.5% above which Mn atoms segregate in Mn-rich nanocrystals, the size of which increases with the nominal Mn concentration x. A similar mechanism has been observed in the GaAsMn DMS [17], in which Mn atoms segregate to the surface even at low growth temperature ($T_S = 430$ K) and low Mn concentration.

3.2. EDXR

The reflectivity profiles (together with their fits) of the $Mn_{0.02}Ge_{0.98}$ and $Mn_{0.06}Ge_{0.94}$ films are shown in Fig. 4 (the critical value k_c of the wave vector below which total reflection occurs, i.e. $k_c = 0.021$ Å^{-1}, is indicated in the figure). The modulation in the reflectivity results from the interference of the X-ray beams reflected at the air-film and film-substrate interfaces [18]. The larger modulation due to the interface between the Ge capping layer and the air is also detectable [19]. The Parratt model [20] for the reflectivity of a film deposited on a substrate was used to fit the experimental data. The general expression for the reflected intensity depends on the scattering length density (SLD), the average thickness, and the surface roughness of the film [21]. In Fig. 4 the red line[1] corresponds to the fit for the Mn_xGe_{1-x} film (more oscillating line) and the blue one to that for the Ge capping film (less oscillating line). The

[1] For interpretation of color in Fig. 4, the reader is referred to the web version of this article.

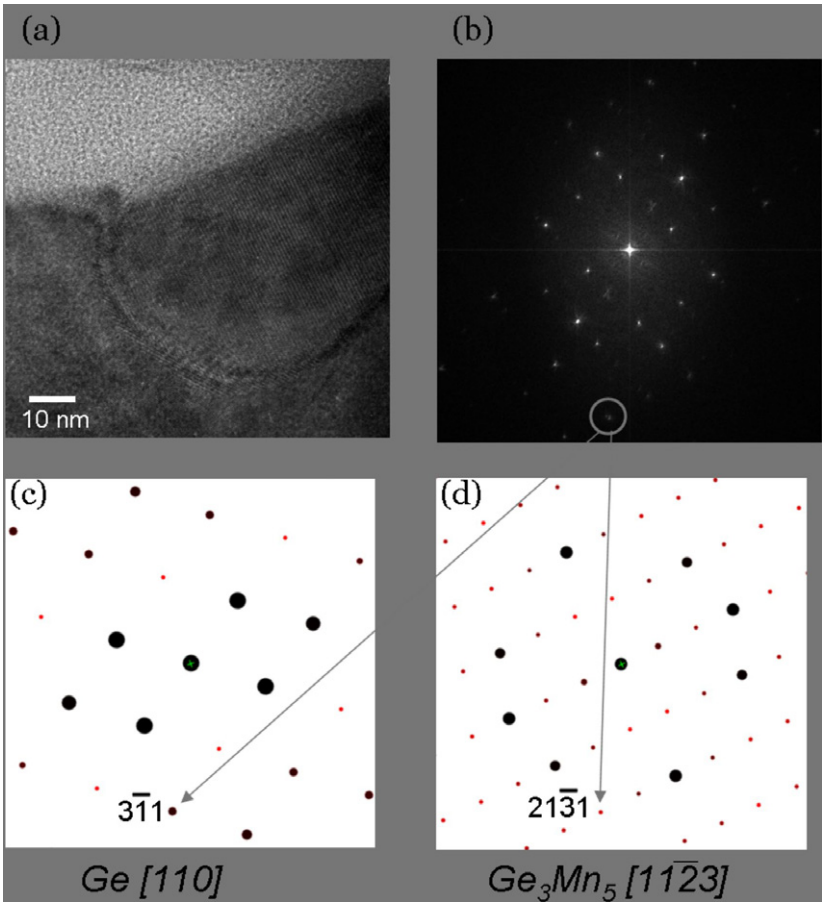

Fig. 3. (a) HRTEM image of a clusters in $Mn_{0.1}Ge_{0.9}$ layer and (b) its calculated Fourier transform. (c) and (d) represent standard diffraction pattern of Ge in [1 1 0] zone axis and Ge_3Mn_5 in [$11\bar{2}3$] zone axis, respectively.

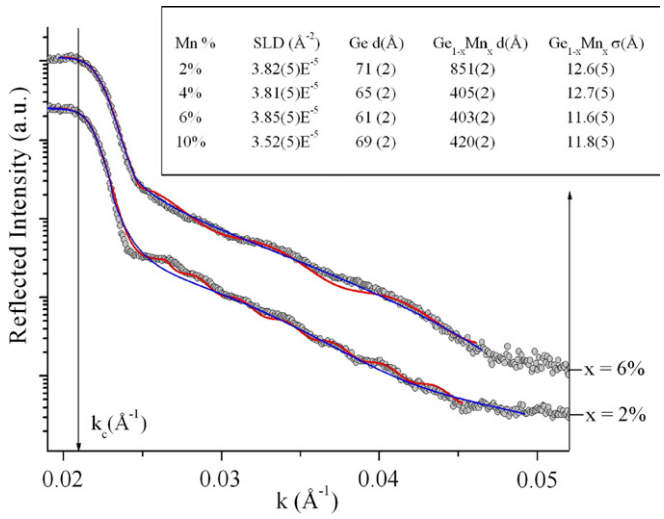

Fig. 4. EDXR spectra on $Mn_{0.02}Ge_{0.98}$, and $Mn_{0.06}Ge_{0.94}$ samples grown at 520 K. The continuous lines are fits to the Parratt model. The arrow indicates the length of k_c the wave vector below which total reflection occurs.

Parratt fit parameters, i.e. the average thickness d (Å), the roughness σ (Å) and the SLD (Å^{-2}) of the Mn_xGe_{1-x} films for the experimental data are given in the inset. The average thicknesses determined in this way are consistent with the values expected from the known deposition conditions.

Considering two films grown with a different Mn concentration, the SLD values are $\rho(Mn_{0.02}Ge_{0.98}) = (3.82 \pm 5) \times 10^{-5}$ Å^{-2} and $\rho(Mn_{0.06}Ge_{0.94}) = (3.85 \pm 5) \times 10^{-5}$ Å^{-2}. These SLD values, which depend also on the sample volume irradiated by the X-ray beam, do not correspond neither to a pure homogeneous Mn_xGe_{1-x} alloy nor to pure Mn–Ge precipitates, but to a combination of two contributions. Thus the EDXR results confirm the presence of two phases (diluted Mn_xGe_{1-x}, and Mn_5Ge_3) in the Mn_xGe_{1-x} film, as observed by HRTEM.

3.3. MOKE

We also investigated by MOKE measurements the magnetic properties of the Mn_xGe_{1-x} films ($0.02 \leqslant x \leqslant 0.1$). We used a polar geometry (**H** perpendicular to the plane) since it provides higher Kerr rotations [typically one order of magnitude higher than the longitudinal geometry (**H** parallel to the plane)].

Fig. 5 shows the ferromagnetic hysteresis loops collected at 12 K and 270 K for the $Mn_{0.1}Ge_{0.90}$ sample. Fig. 6a and b give the remanence of the Kerr rotation and the coercive

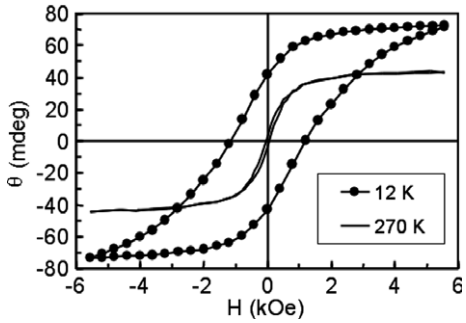

Fig. 5. MOKE hysteresis loop at 12 K and 270 K for the $Mn_{0.1}Ge_{0.9}$ sample.

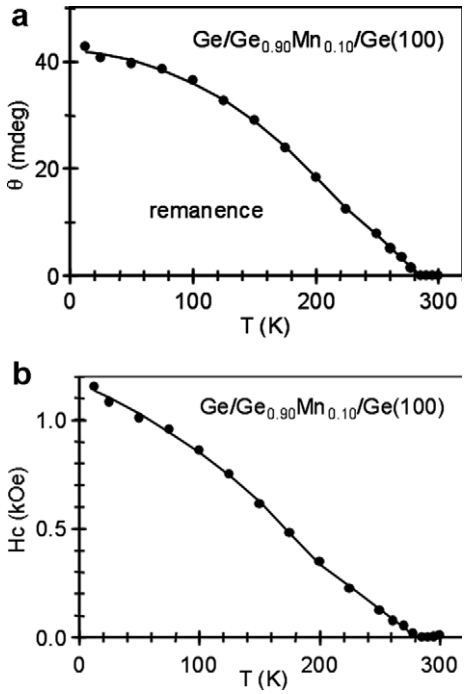

Fig. 6. Temperature dependence of the MOKE remanence (a) and of the coercive field (b) for the $Mn_{0.1}Ge_{0.9}$ sample. The line is a guide to the eye.

field as a function of temperature in the 13–300 K range. From Fig. 6a, we derive a Curie temperature $T_C \approx 280$ K. All the Mn_xGe_{1-x} samples exhibit a magnetic signal. This magnetic signal is due to the precipitates present in the films (see also Refs. [10,13]). The diluted Mn_xGe_{1-x} films show paramagnetic behavior as measured by SQUID magnetometry and described in Ref. [13]. The signal increases with increasing Mn concentration and it reaches a maximum for $x = 0.1$. When the nominal Mn concentration x in the Mn_xGe_{1-x} film is above 0.1, the magnetic signal drops due to the formation of Mn clusters, which destroy the ferromagnetism because of their antiferromagnetic properties.

4. Conclusions

In conclusion, we have reported the structural and magnetic properties of Mn_xGe_{1-x} alloys, with $0.02 \leqslant x \leqslant 0.1$, grown on Ge(0 0 1) substrates held at 520 K, obtained from HRTEM, SAED, EDXR, and MOKE measurements. HRTEM images and SAED patterns show that all the samples, the thicknesses of which have been determined by EDXR in an independent way, contain Mn_5Ge_3 clusters incorporated in the epitaxial Mn_xGe_{1-x} film. The size of these clusters increases with the Mn concentration. MOKE experiments showed ferromagnetic order in all the Mn_xGe_{1-x} films with $T_C \approx 280$ K.

Acknowledgements

The authors are grateful to S. Priori and M. Capozi for their appreciable technical help. The financial support by the Italian CNR/MIUR (FISR: ''Nanotecnologie per dispositivi di memoria ad altissima densità'' and FIRB: ''Nanotecnologie e nanodispositivi optoelettronici e spintronici'') is gratefully acknowledged.

References

[1] S.A. Wolf, D.D. Awschalom, R.A. Buhrman, J.M. Daughton, S. von Molnár, M.L. Roukes, A.Y. Chtchelkanova, D.M. Treger, Science 294 (2001) 1488.
[2] T. Dietl, H. Ohno, F. Matsukura, J. Cibert, D. Ferrand, Science 287 (2000) 1019.
[3] J. Inoue, S. Nonoyama, H. Itoh, Phys. Rev. Lett. 85 (2000) 4610.
[4] A. Chattopadhyay, S. Das Sarma, A.J. Millis, Phys. Rev. Lett. 87 (2001) 227202.
[5] J. Kanamori, K. Terakura, J. Phys. Soc. Jpn. 70 (2001) 1433.
[6] J.-S. Kang, G. Kim, S.C. Wi, S.S. Lee, S. Choi, S. Cho, S.W. Han, K.H. Kim, H.J. Song, H.J. Shin, A. Sekiyama, S. Kasai, S. Suga, B.I. Min, Phys. Rev. Lett. 94 (2005) 147202.
[7] Y.D. Park, A.T. Hanbicki, S.C. Erwin, C.S. Hellberg, J.M. Sullivan, J.E. Mattson, T.F. Ambrose, A. Wilson, G. Spanos, B.T. Jonker, Science (2002) 295.
[8] N. Yamada, K. Maeda, Y. Usami, T. Ohoyama, J. Phys. Soc. Jpn. 55 (1986) 3721.
[9] S. Cho, S. Choi, S.C. Hong, Y. Kim, J.B. Ketterson, B.-J. Kim, Y.C. Kim, J.-H. Jung, Phys. Rev. B 66 (2002) 033303.
[10] C. Bihler, C. Jaeger, T. Vallaitis, M. Gjukic, M.S. Brandt, E. Pippel, J. Woltersdorf, U. Gösele, Appl. Phys. Lett. 88 (2006) 112506.
[11] Y.D. Park, A. Wilson, A.T. Hanbicki, J.E. Mattson, T. Ambrose, G. Spanos, B.T. Jonker, Appl. Phys. Lett. 78 (2001) 2739.
[12] L. Morresi, J.P. Ayoub, N. Pinto, M. Ficcadenti, R. Murri, A. Ronda, I. Berbezier, Mat. Sci. Semic. Proc. 9 (2006) 836.
[13] P. De Padova, J.-P. Ayoub, I. Berbezier, J.-M. Mariot, A. Taleb-Ibrahimi, M.C. Richter, O. Heckmann, A.M. Testa, D. Fiorani, B. Olivieri, S. Picozzi, K. Hricovini, Surf. Sci. 601 (2007) 2628.
[14] E. Sawatzky, J. Appl. Phys. 42 (1971) 1706.
[15] C. Zeng, S.C. Erwin, L.C. Feldman, A.P. Li, R. Jin, Y. Song, J.R. Thompson, H.H. Weitering, Appl. Phys. Lett. 83 (2003) 5002.
[16] R. Felici, F. Cilloco, R. Caminiti, C. Sadun, V. Rossi, Patent No. RM 93 A 000410, Italy, 1993.
[17] K.W. Edmonds, N.R.S. Fadley, R.P. Campion, C.T. Foxon, B.L. Gallagher, T.K. Johal, G. van der Laan, M. MacKenzie, J.N. Chapman, E. Arenholz, Appl. Phys. Lett. 84 (2004) 4065.
[18] P. De Padova, A. Generosi, B. Paci, V. Rossi Albertini, P. Perfetti, C. Quaresima, B. Olivieri, M.C. Richter, O. Heckmann, F. D'Orazio, F. Lucari, K. Hricovini, Surf. Sci. 600 (2006) 4190.
[19] B. Paci, A. Generosi, V. Rossi Albertini, E. Agostinelli, G. Varvaro, D. Fiorani, Chem. Mater. 16 (2004) 292.
[20] L.G. Parratt, Phys. Rev. 95 (1954) 359.
[21] X.L. Zhou, S.H. Chen, Phys. Rep. 257 (1995) 224.